ME 2240

Final Project

Owen Calderwood, Nolan Chanda, Jimmy Pare, Camden Piper

Prof. Dubief

Abstract—Snow storage over the summer months is a promising method to maintain ski areas in good condition when natural snowfall is sparse. The goal was to evaluate how thermal insulation and phase shift affect heat transfer and snow preservation. Task 1 used simulations to show that R-value alone was not responsible for effective storage. In Task 2, several simulations were completed to estimate the phase shift of heat entering the building, total heat loss, and the effects of weather and different insulation types on heat transfer. To maintain the inside of the building at 0 degrees Celsius throughout the summer, an average cooling power of 35 kW was required with peaks around 44 kW. Increasing the phase shift of heat flux entering the outer and inner surfaces of the walls proved beneficial to regulating the facility's temperature. Task 3 calculated snow melt from thermal input to assess whether the pile size was large enough. Task 4 examined a cooling system using pond water to reduce solar heat on the wall with most heat input, recovering waste heat as 30℃ water. Results from the first task found that the insulation's density and heat capacity affected the phase shift, responsible for heat storage. Doubling the insulation thickness increased phase shift, a positive attribute for this study, however cost had to be considered. Results demonstrated the importance of phase shift and integrated thermal design for seasonal snow storage. Results from the third task predicted that 4016 cubic meters of snow would remain at the end of October if a 14 cm thick layer of wood insulation was utilized. An estimate of 79 MWh of total energy usage for cooling was calculated as well as a maximum power of 1127 kW. Results for the fourth task included a required heat extraction of $5.64\frac{W}{m^2}$, which corresponded to a water transport pipe length of 22.018 meters and pumping power input of 0.00102 W.

Keywords—*Heat Transfer, snow storage, energy reduction*

1. Introduction

This study evaluated the insulation performance of materials with equivalent R-values but differing thermal mass, showing that while steady-state heat transfer was identical, transient or cyclic temperature variations revealed notable differences in thermal behavior. In this study, transient weather data was used to run heat transfer simulations to optimize a snow storage facility design.

Climate change has had a profound impact on the ski industry throughout the world. A 2024 study **mitterwallner2024global** showed a consistent reduction of annual snow cover days from 1981 to 2010 in seven major mountains sampled across the world. The authors also used different global warming models to predict the further decrease of annual snow days by more than 50% of historic baselines. To adapt to these changes, ski resorts around the world have implemented snow making. In fact, all ski areas in the Northeast, Southeast and Midwest ski regions of the United States now employ snow-making **scott2007climate**. Snow-making is important for the operation of ski resorts, but it is not enough to guarantee snow. If conditions are not right for snow making, alternative methods, such as snow storage, are the only option. Snow storage has been utilized for centuries, used primarily as a method of cooling food and houses **grunewald2018snow**. Snow storage is now being used by ski resorts to adapt to Earth's changing climate. Winter sporting events, such as the 2014 Olympic Games held in Sochi, Russia, depended on stored snow **grunewald2018snow**. In this experiment, numerical simulations were manipulated to evaluate a summer snow storage facility design. The vision was an insulated facility large enough to store a snow pile of dimensions 20m ×70m ×5m with enough head space to allow for Nordic skiing on the snow pile during the summer. During the coldest days of February and March, artificial snow was made using HKD air/water guns attached to the ceiling of the facility. Large fans ran down the length of the building with open garage doors to maintain a cold temperature during the cold months. During the warm months, when outdoor skiing was not possible, a small course inside the facility was available for Nordic skiers. Day passes were sold to help cover electricity and construction costs. In late November, the snow was pushed out of the facility to form a large outdoor course. Large garage doors located on the two ends of the facility allowed for easy access to the snow with a bulldozer. To maintain an internal temperature of zero degrees Celsius, air conditioning was implemented. Solar panels located on the roof helped power the air conditioning, as well as reducing heat transfer. The system was optimized such that enough snow remained for a one-kilometer course with a width of eight meters and a depth of half a meter.

The walls of the building were designed with $R22$ or $R30$ insulated concrete to form a layer of insulation with thin wood paneling. To investigate the thermal performance of various materials, a simple simulation was conducted. It evaluated heat transfer through different wall compositions using a sinusoidal temperature variation to model a simplified day-night cycle. A wall configuration supported by our simple model was evaluated using a far more complex simulation that calculated heat transfer (q'') through walls as a function of weather data. This accounted for all the modes of heat transfer present at the outside surfaces of the facility. This model also accounted for heating and cooling via radiation, convective heating and heat transfer due to rain using weather data collected from April to October of 2020 in Essex Junction Vermont. Radiation from the sun heated the exposed surfaces of the facility. Solar panels located on the roof absorbed a portion of this heat and converted it into electricity, slightly reducing the solar radiation heat transfer. As a result of solar radiation, the exposed surfaces became hotter than the surrounding atmosphere, meaning some heat was then radiated back away from the facility. Convective heat transfer, a function of wind speed and air temperature, heated the building. Rain could provide cooling on hot days and heating on cold days. Although air conditioning inside the building maintained an internal temperature of zero degrees Celsius, all the heat through the facility walls was assumed to go into melting the top surface of snow, allowing for an estimate of snow depth loss over time as a function of the weather data. The total heat transfer through the walls was calculated by multiplying the heat flux per unit area ($q\varepsilon$) by the area of the walls and roof of the facility. It was assumed that the bottom wall was in a state of permafrost, resulting in no heat penetration. If the estimated snow depth did not amount to enough snow for a one-kilometer course, accounting for losses during transportation, the wall configuration needed to be adjusted. The total amount of energy in kilowatt hours needed to maintain a temperature of zero degrees Celsius was estimated as well as the maximum energy needed over the entire period of investigation. Lastly, the feasibility of an additional cooling method involving pumping water from a nearby pond to the roof of the facility was investigated.

2. Methods

2.1. Governing equations

All equations used in our codes were defined and the missing code for flux `qpp_x1` for weather simulation was implemented as shown below.

Transient simulations of heat transfer in the walls under investigation solved the 1D heat equation

$$\rho C_p \frac{\partial T}{\partial t} = \frac{\partial}{\partial x} k \frac{\partial T}{\partial x} \tag{1}$$

where the density ρ, specific heat C_p and thermal conductivity k were material dependent but their variations with temperature were assumed to be negligible. The boundary conditions for Eq. (1) with boundary conditions at either end ($x = 0$ or $x = L$) could be one of the following:

Dirichlet, where temperature was defined by the user:

$$T(x=0,t)=T_{x_0} \quad \text{or} \quad T(x=L,t)=T_{x_1}$$

Or Neumann, where flux was defined by the user:

$$-k\frac{\partial T}{\partial x}\bigg|_{x=0}=q''_{x_0} \text{ or } -k\frac{\partial T}{\partial x}\bigg|_{x=L}=q''_{x_1}$$

This study used the values of $x=0$ as $x0$ and $x=L$ as $x1$.
On the outside surface, the code was:

```
while (t < tend):
    qpp_x1 = -0.8*weatherfct.sun_irradiation(t) # radiation going into the building
    qpp_x1 += weatherfct.qpp_skyradiation(t, T[-1]) # radiation going out
    qpp_x1 += weatherfct.qpp_outsideconvection(t, T[-1], Lplate=wall_length)  # convection cooling
    qpp_x1 += weatherfct.qpp_rain(t, T[-1])    # rain cooling
```

Code 1. Python code of heat fluxes on outer surface of building.

To estimate the decreasing height of the snow pile, the following equation was used

$$\frac{dH}{dt}=\frac{min(q_{wall,x0}(t),0)}{\rho_{snow}A_{top}h_{l,snow}} \tag{2}$$

where H was snow pile height, ρ was density, A_{top} was area of the snow, and $h_{l,snow}$ was convection coefficient.

To estimate the head loss in a pipe, the Darcy–Weisbach equation must be solved

$$h_f=\frac{fLv^2}{2gD} \tag{3}$$

Where L is pipe length, v is fluid velocity, g is gravitational acceleration, D is pipe diameter, and f is friction factor, given as

$$f=\frac{64}{Re} \tag{4}$$

for laminar flow. Pumping power can be determined with

$$P=\rho gAvh_f \tag{5}$$

Where P is pumping power and A is cross-sectional area of the pipe.

2.2. Climate data

The climate data used in simulations was collected from April to October of 2020 in Essex Junction Vermont. Wind speed, wind direction, cloud cover as a percentage, dew point temperature, relative humidity, precipitation, sun irradiation, and minimum maximum and average temperature were recorded every 15 minutes.

3. Heat insulation *vs* heat storage

3.1. Description of experiment

By using numerical simulations, deviations from steady-state assumptions were observed when examining systems changing with time. In this case, this experiment showed that reducing the R-value of insulation in a wall was not the only deciding factor in understanding the entire system's heat transfer. This simulation studied the transient heat transfer between walls with different insulation compositions. Table 1 shows the thermal properties of the relevant materials in this experiment.

Table 1. Thermal properties of materials

Material	ρ (kg/m^3)	C_p (J/kg.K)	k (W/m.K)
Cast Concrete	2400	880	1.4
Wood Siding	550	1800	0.14
Compressed Wood Fiber	1000	1800	0.03
XPS Polystyrene Fiber	33	1400	0.03

Three different wall compositions were studied. The first was the base wall without any insulation. This included 10 cm of cast concrete being closest to the interior and 1 cm of wood siding on the exterior. The second wall included compressed wood fiber between the two existing layers for insulation. The third wall, similar to the second, used XPS polystyrene fiber as insulation.

The initial steady-state models led to the finding of values of q''_{x1} for each wall composition. The numerical simulations were verified using thermal resistivity, and then a transient simulation was applied. This simulation applied an oscillatory function as a simplification of the day-night cycle. The function at x1 was as follows:

$$q''(x=L)=q''_{x1}\cos(2\pi\omega t) \tag{6}$$

where q''_{x1} was an estimated value based on the findings in the steady-state analysis, and $\omega=1/(24\cdot 3600)$, the inverse of one day.

3.2. Results

The previously mentioned numerical simulations for steady-state analysis were studied. For the configuration without insulation, $q''_{x1}=100$ was implemented. For the remaining two insulation configurations, $q''_{x1}=50$ was implemented. The relevant results are shown below in Table 2.

Table 2. Heat flux and R-values of each wall.

Configuration	q''_{x1} (W/m^2)	R_{theory}	R_{sim}	R_{thm}
No insulation	-112.439	1	1.016	0.816
Wood insulation	-10.853	11	10.530	10.340
XPS insulation	-10.853	11	10.530	10.430

These values were then substituted into Eq. (6) to form the transient simulations for each wall composition. The transient heat flux on each boundary of x0 and x1 was then studied throughout a period of 24 hours. Fig. 1 shows the simulation for each wall composition.

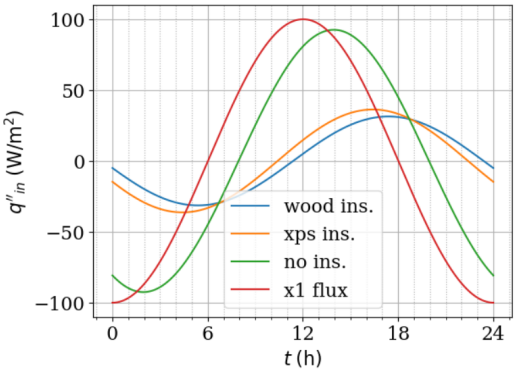

Figure 1. Interior wall heat flux ($x=0$) for different wall compositions compared to input flux load (x1 flux). The plot shows the last 24 hours of a 40 day simulation.

Furthermore, the amount of heat flux per day was modeled as a bar chart, as seen in Fig. 2.

These two figures represent the purpose of this study. From Table 1, the thermal conductivity (k) of both the wood and XPS insulation was

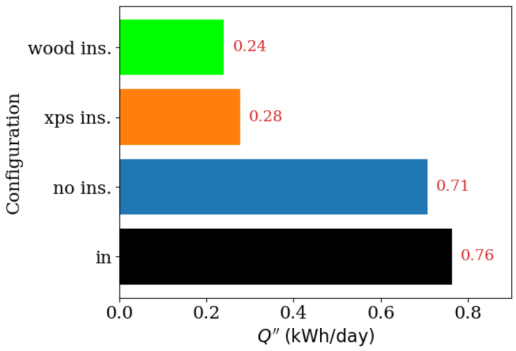

Figure 2. Total heat flux per day for each wall configuration.

the same value. Table 2 also showed the study and thermal resistivity calculations resulting in the same R-values. Fig. 1 showed the wood insulation having a larger phase shift from the x1 flux compared to the XPS insulation. This was exemplified in Fig. 3.

The phase shift was different between the wood and XPS because of the different densities and specific heat capacities. From Table 1, the wood insulation had a density of 1000 kg/m^3, compared to XPS's density of 33 kg/m^3. Similarly, the wood insulation had a heat capacity of 1800 J/kg.K, compared to XPS's density of 1400 J/kg.K. The phase shift difference explained the difference in values seen in Fig. 2. The wood insulation configuration found the heat flux to be $Q'' = 0.24$ kWh/day. The XPS insulation found the heat flux to be slightly higher, at $Q'' = 0.28$ kWh/day.

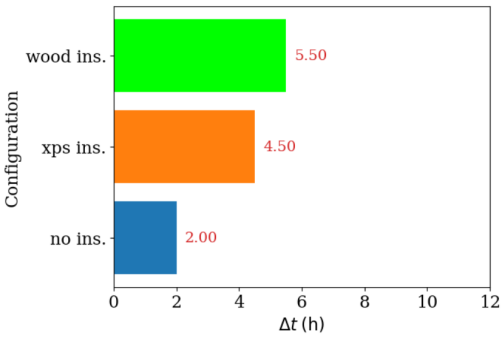

Figure 3. Phase shift from x1 flux for each wall configuration.

Fig. 3 gave numerical values for the phase shift for each wall configuration. Heat insulation prevented heat flow between two boundaries, whereas heat storage absorbed heat, stored it, and then released the heat over time. Materials with higher densities and heat capacities had larger phase shifts, and were therefore better for heat storage.

When the insulation layers were doubled in thickness, the heat flux (Q'') and phase shift (Δt) were affected accordingly, as seen in Fig. 4.

Doubling the insulation thickness decreased the daily heat flux in each insulated configuration. The wood insulation configuration saw a 50.0% decrease in heat flux, which resulted in the phase shift increasing by 45.5%. The XPS insulation configuration saw a 32.1% decrease in heat flux, resulting in a 33.3% increase in phase shift. Doubling the insulation thickness also doubled the difference in phase shifts between the wood and XPS insulations.

While doubling the insulation was clearly effective in decreasing the heat flux and increasing the phase shift, the cost to add this added insulation had to be accounted for. The application of this topic depended on the amount of insulation needed. For this study, it was more useful to look at wall configurations with longer phase shifts, so cost management was extremely important.

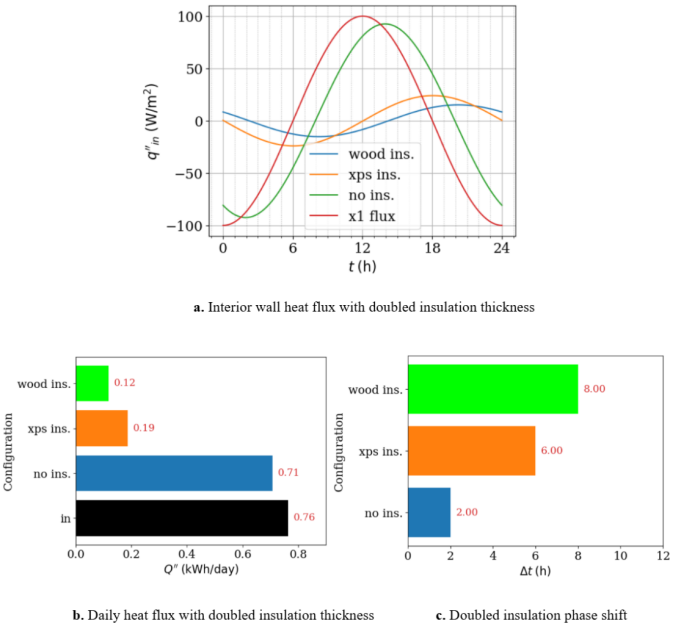

a. Interior wall heat flux with doubled insulation thickness

b. Daily heat flux with doubled insulation thickness

c. Doubled insulation phase shift

Figure 4. Transient simulation results with doubled insulation thickness.

4. Heat rate from weather data

The heat fluxes across different control volumes were calculated using numerical methodology. Without internal cooling or insulation, the heat rates at the inner and outer surfaces of the snow storage facility were shown in the figure below, not considering radiation leaving the building, cooling via convection, and cooling by rain. The blue line was the heat flux at the outer surface of the walls, and the red line was the heat flux at the inner surface. In this simulation, the wall consisted of concrete and wood paneling, without insulation.

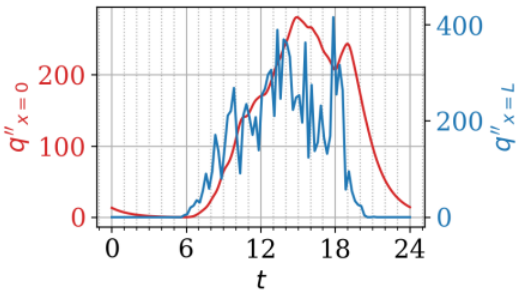

Figure 5. Heat fluxes at the inner and outer surfaces of the wall, only considering irradiation.

Due to the thermal inertia of the wall, the heat flux at the inner surface experienced fewer fluctuations than at the outer surface. Additionally, a phase shift between the heat fluxes was observed, with the heat flux at the outer surface leading the heat flux on the inner surface by approximately 1-2 hours.

Although Figure 5 gave a general idea of the behavior of the fluxes, a more accurate simulation was made by considering heat loss due to radiation, convection, and cooling by rain. Figure 6 compared the heat fluxes without these other factors (dotted) to the heat fluxes with radiation leaving the building, convective cooling, and cooling by rain.

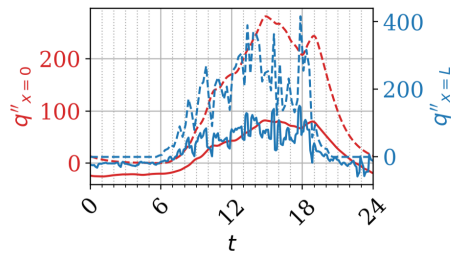

Figure 6. Heat fluxes with radiation, convection, and rain compared to heat fluxes without.

The cooling from rain, convection from the wind, and the building radiating to the surroundings caused substantial decreases in heat fluxes on both surfaces. The oscillations in the heat flux on the wood siding also decreased in magnitude due to these factors.

Figure 7 was from the same simulation as Figure 6 (considering real world factors), but with the time scale extended to 40 days. The blue line represented the heat flux at the outer surface and the red line was the heat flux at the inner surface.

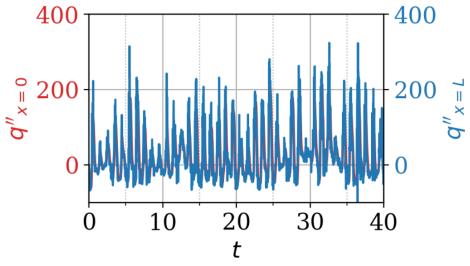

Figure 7. Heat fluxes at the inner and outer surfaces of the building during 40 day period.

Due to the increased time scale, the differences in heat fluxes at the inner and outer surfaces were not as visible in Figure 7 as previous figures. Extreme fluctuations in heat transfer were observed between day and night, varying with weather conditions.

One other option considered in simulation was adding insulation between the concrete and wood paneling. Figure (11) showed the heat fluxes on each surface throughout one day after adding a layer of insulation with thermal conductivity .04 $\frac{W}{m*K}$.

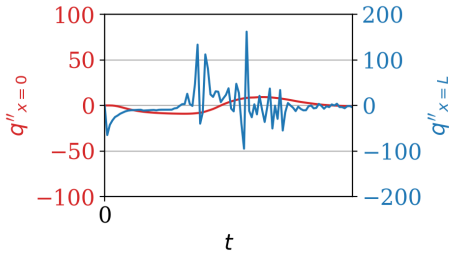

Figure 8. Heat fluxes on inner and outer surfaces with insulation.

Adding insulation greatly decreased the amount of heat entering the building and also slightly increased the phase shift to about 2 hours. This simulation indicated that it would be extremely beneficial to add a layer of insulation to the walls of the snow storage building.

While not studied in this simulation, using a material with a higher thermal mass would increase the phase shift of heat transfer. By using a material like compressed wood fiber, a much larger phase shift between the inner and outer surfaces of the building could be obtained. This would prove to be extremely beneficial for summer snow storage because the facility would passively regulate its own temperature. With a higher thermal mass, the building would effectively be cooling itself for the first several hours of the day.

Using the data for the heat flux at the inner surface of the building, an estimate for the cooling power required was obtained. Using the expression shown in Equation (7) and a trapezoidal sum on the data from Figure 11 resulted in a 35 kW mean cooling requirement with a 44 kW required max load to keep the building at 0 degrees Celsius.

$$q''_{\text{cooling}} = \frac{1}{t_{\text{total}}} \int_0^{t_{\text{total}}} q''_{x=0}(t)\, dt \tag{7}$$

If there was no temperature control, the building would slowly increase in temperature until a steady state temperature was reached between 0 degrees Celsius and the outside temperature. This would result in the snow melting fairly quickly and likely not lasting through the summer.

5. Snow melt

With walls composed of 10 cm of cast concrete, 10 cm of compressed wood fiber and 1 cm of wood siding, the heat rate entering the open cavity of the building was used to estimate snow melt. It was estimated that $3776m^3$ of snow would remain at the end of October. This was not enough snow for a one-kilometer course. The simulation was run again with 14 cm of compressed wood fiber. Now estimating that $4016m^3$ of snow would remain at the end of October. This met the $4000m^3$ requirement for snow volume.

To determine this value, the heat flux of snow(qpp_snow) was calculated by multiplying the heat flux entering the roof (qpp_wall) by the ratio of the total wall area over the top snow surface area. The heat flux of the walls was assumed to be the same as the heat flux through the roof and the heat flux through the ground was assumed negligible due to a permafrost state. Bounds of $-\infty$ and 0 were set to wall heat flux data meaning all heat flux entering the cavity melted the snow but heat flux leaving the cavity did not cool the snow.

$$\texttt{qpp\_snow} = \texttt{np.clip(wall\_d.qpp\_x1, a\_min=None, a\_max=0)} \cdot \frac{\texttt{A\_wall\_total}}{\texttt{A\_snow}}$$

The above equation was used in the python simulation.

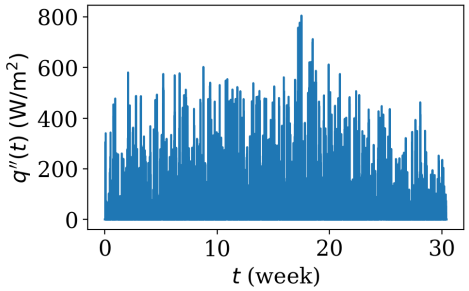

Figure 9. This figure shows the heat flux in (W/m^2) traveling into the top surface of the snow versus time in weeks.

Height loss of the snow pile was determined by taking the integral of the snow heat flux (qpp_snow) divided by the latent heat transfer coefficient (h_l) and the snow density (rho_snow). The following equation was used in python to determine loss in height of the snow pile ($depth\_loss$). The final snow height was 2.7 m.

$$\texttt{depth\_loss} = \texttt{cumulative\_trapezoid}\left(\frac{\texttt{qpp\_snow}}{\texttt{h\_l} \cdot \texttt{rho\_snow}}, \texttt{wall\_d.t}\right)$$

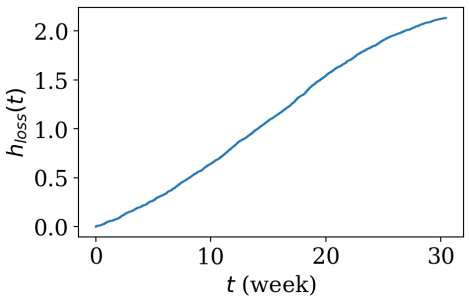

Figure 10. This figure shows the loss in height of the snow pile versus time.

To calculate the volume of the snow pile with time, the loss in snow height multiplied by the top surface area was subtracted from the initial volume of the snow pile. The final snow volume was $4016m^3$.

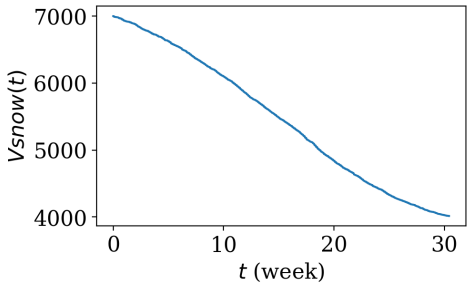

Figure 11. This figure shows the change in volume of the snow pile versus time.

By integrating the total heat rate through the facility walls, a total energy consumption of 79 MWh was calculated. This was a tremendous amount of energy. The maximum cooling power calculated in the simulation was 1127 kW. No cooling was needed for 64 % of the simulated period.

6. Feasibility of cooling of extreme events

On the hottest days, the outside temperature likely reached approximately $35°C$. However, concrete that had been exposed to solar radiation for a prolonged duration could reach $62°C$**zhang2023thermal**. A wall at this temperature accelerated the heat transfer into the snow storage building and required excess cooling to maintain an indoor temperature of $0°C$. The relation $q'' = \frac{\Delta T}{R''}$ was employed. Using an R-value per unit area of $11\frac{m^2K}{W}$, there was a heat addition of $5.64\frac{W}{m^2}$ to the indoors. Therefore, this amount of heat had to be removed from the wall, which was done by pumping cooling water from a nearby pond. The heat flux found above was equated to $q'' = h(T_{wall} - T_{pond})$ with Nusselt number $Nu = \frac{hL}{k_f}$. The pipe to be used was designed by defining some parameters concerning the pipe flow. It was assumed that the pipe exhibited laminar flow and constant heat flux since only one temperature was being examined. Therefore, a Nusselt number of $Nu = 4.36$ was estimated. If the pond water was at a temperature of $15°C$, then its thermal conductivity was about $k_f = 0.606\frac{W}{m}$. Assuming a temperature difference of $\Delta T = 62°C - 15°C$, the pipe length required was $L = 22.018m$. Then, fluid velocity is assumed to be $0.04\frac{m}{s}$ and pipe diameter 0.05 meters. Pumping the water resulted in a head loss of 0.00132 meters and therefore a required input of 0.00102 W.

7. Conclusion

This study sought to evaluate thermal insulation and snow storage and apply these principles for large-scale snow storage over warmer months. Full utilization included enough snow for a small indoor ski facility. The first part of the study involved understanding the difference between heat insulation and heat storage between different materials. Understanding that transient heat transfer was affected by not only R-value, but also by the phase shift was crucial in the further steps of this study. Wood insulation had a phase shift of $\Delta t = 5.5$ hr, with $Q'' = 0.24$ kWh/day. The XPS insulation had a slightly lower phase shift value of $\Delta t = 4.5$ hr, resulting in a heat flux of $Q'' = 0.28$ kWh/day. This part looked into heat storage further by doubling the insulation layer thickness. The resulting phase shifts for wood and XPS became 8 hrs and 6 hrs respectively. This was more applicable to the snow storage objective, but costs had to be considered.

The second part of the study focused on experimenting with different insulation parameters to optimize phase shift so that an inside temperature of $0°C$ could be maintained. After multiple simulations recreating real-world weather patterns, a 35 kW mean cooling power was calculated with peaks up to 44 kW.

The third part of the study looked at predicting snow melt and gauging whether enough snow would remain in the building to permit use by skiers. With a thickness of 14 cm of wood insulation it was predicted that 4016 cubic meters of snow would remain at the end of October. An estimate of 79 MWh of total energy usage for cooling with a maximum power of 1127 kW was calculated.

The fourth part of the study explored options for additional cooling when the outside temperature was at its hottest and the sun was strong. It was determined that $5.64\frac{W}{m^2}$ of heat had to be removed from the building. This was done by pumping cooling water from a nearby pond. A pipe sufficient for this purpose to obtain the correct convection coefficient had to be 22.018 meters. Transporting this water required an input pumping power of 0.00102 W.

8. Who did what?

Owen Calderwood : Introduction, Snow Melt
Nolan Chanda : Heat insulation vs heat storage, Conclusion
Jimmy Pare : Weather simulation of snow storage facility.
Camden Piper : Feasibility of cooling of extreme events, Abstract

References

1. Scott, D., & McBoyle, G. (2007). *Climate change adaptation in the ski industry*. Mitigation and Adaptation Strategies for Global Change, 12, 1411–1431. Springer.
2. Grünewald, T., Wolfsperger, F., & Lehning, M. (2018). *Snow farming: Conserving snow over the summer season*. The Cryosphere, 12(1), 385–400. Copernicus GmbH.
3. Zhang, Z., Hamid, M., Khan, S., Asif, M., Liu, Y., Ma, X., & Liu, J. (2023). *Thermal performance and environmental assessment of a novel passive cooling strategy for building applications*. Heliyon, 9(6), e15432. Elsevier.

